The Talamancan Central America region has been a major staging ground ɔr salamander evolution. The bulk of the salamander fauna can be traced ultiıately to more northern zones, but at least one major clade, *Oedipina,* may ave originated and undergone its most dramatic radiation here. Importantly, ıis region supplied the lineages that successfully occupied South America hen that continent became physically accessible.

ıcknowledgments

have summarized the results of forty years of investigations, by me and my ose associates, in Costa Rica. Jay Savage and Arden Brame encouraged me to udy tropical salamanders, and Pedro León, Rodrigo Gámez, the late Douglas obinson, Luis Diego Gómez, Dan Janzen, and Federico Bolaños have been ırticularly helpful in the course of my work in Costa Rica. Among many assoates who have worked with me on Costa Rican salamanders I particularly ıank Arden H. Brame, the late James F. Lynch, James Hanken, David Good, 'avid Cannatella, Kiisa Nishikawa, Gerhard Roth, Andes Collazo, Thomas A. Vake, Marvalee H. Wake, Nancy Staub, Stanley Sessions, Elizabeth Jockusch, Iario García-París, Karen Lips, and Sharyn Marks. Three reviewers made ɔmments that improved the chapter. My work was long sponsored by the Naonal Science Foundation and the Museum of Vertebrate Zoology.

Pages 81-101 *in* Maureen A. Donnelly, Brian I. Crother, Craig Guyer, Marvalee H. Wake, & Mary E. White (editors), Ecology & Evolution in the Tropics. A Herpetological Perspective. The University of Chicago Press: Chicago & London. xv + 675 pages.

4

On the Enigmatic Distribution of the Honduran Endemic *Leptodactylus silvanimbus* (Amphibia: Anura: Leptodactylidae)

W. Ronald Heyer, Rafael O. de Sá, and Sarah Muller

Most species of the frog genus *Leptodactylus* occur in South America, and all authors who have treated the zoogeography of the genus have concluded that it originated somewhere in South America (e.g., Savage 1982). Savage (1982, 518) summarized the historical herpetofaunal units of the Neotropics as follows: "All evidence points to an ancient contiguity and essential similarity of a generalized tropical herpetofauna that ranged over tropical North, Middle, and most of South America in Cretaceous-Paleocene times. Descendents of this fauna are represented today by the South and Middle American tracks (Elements). To the north of this fauna ranged a subtropical-temperate Laurasian derived unit, today represented by the Old Northern Element (track). By Eocene, northern and southern fragments of the generalized tropical units had become isolated in Middle and South America, respectively. Differentiation in situ until Pliocene produced the distinctive herpetofaunas that became intermixed with the establishment of the Isthmian Link."

The paleogeographical data available to Savage were consistent with the preceding statement. New geological information over the past 20 years has clarified some aspects of the historical relationships between landmasses now comprising Middle and South America, but there is still not a single paleogeographical set of reconstructions accepted by all workers. Iturralde-Vinent and MacPhee (1999) presented cogent arguments that a detailed paleogeographic

construction of the Caribbean region (as well as Middle America) will likely never be possible because of the nature of the geological data themselves.

The importance of Savage's biogeographic work in Middle America (e.g., Savage 1982) lies in the conclusion that there has been a relatively old radiation of the herpetofauna in Middle America that developed in situ. The available data do not unambiguously determine how and when the ancestors of this radiation were established in Middle America (see, for example, the introductory sections in Iturralde-Vinent and MacPhee 1999).

The herpetofaunal fossil record for the late Cretaceous through the Pliocene is limited for the New World (Estes and Báez 1985). However, taken at face value (that is, the oldest known fossils represent the first appearances of the taxa in the region), the fossil data suggest that there was limited, ongoing exchange between Middle and South America from the Eocene until the establishment of the Isthmian Link (Estes and Báez 1985, fig. 2). Most of the recent works that include Middle American paleogeographic reconstructions indicate that there is no overwhelming evidence of a land bridge or an island-arc land bridge between North and South America from the Paleocene until the Pliocene establishment of the Panamanian Isthmian Link. However, there is some evidence to suggest that there may have been a brief Panamanian land bridge in the Miocene (e.g., Iturralde-Vinent and MacPhee 1999).

A conservative summary relative to understanding *Leptodactylus* distributions includes the following two elements:

1. Sometime during the Miocene to Eocene, representatives of the South American tropical herpetofauna were on landmasses that now constitute Middle America and began an in situ radiation that resulted in most of the species that now occur in Middle America. An example of this radiation is the many species representing groups or genera of frogs of the family Hylidae endemic to Middle America (see Campbell 1999). How the ancestors of the Middle American radiation arrived on the old Middle American landmasses is not clear.
2. Formation of the Isthmian Link in the Pliocene then allowed two-way dispersals of the Middle American radiation with the South American herpetofauna. Any transport of propagules between the times when the ancestors of the Middle American radiation were in place and the formation of the Panamanian Isthmian Link must have been via overwater dispersal.

The patterns of relationships among the species of *Leptodactylus* that occur in Middle America are rather different from those of some of the Middle American hylid frogs, suggesting different zoogeographic histories and patterns. For example, all species of the hylid genera *Duellmanohyla* and *Ptychohyla* occur only in Middle America, and the relationship of these frogs to other hylid frog

groups is unclear. This pattern fits Savage's (1982) model for the Middle American radiation well. However, the Middle American *Leptodactylus* species exhibit a different pattern.

All but one known species of *Leptodactylus* in Middle America have either a widespread distribution in South America, with a modest distribution in Middle America, or extensive geographic distributions in Middle America and occur either along lowland Pacific coastal Colombia and Ecuador or Caribbean coastal Colombia and Venezuela. Within this general characterization, there are four different distribution patterns among Middle American *Leptodactylus* species.

1. *Leptodactylus fuscus,* with a widespread distribution in South America, only extends as far north as the Panama Canal region in Panama.
2. *Leptodactylus insularum* and *L. pentadactylus* each have moderate distributions in Middle America and apparently have close sister-group relationships with species having distributions in South America (Heyer 1998, 2).
3. *Leptodactylus labialis, L. melanonotus,* and *L. poecilochilus* have moderate to extensive distributions in Middle America and have no obvious sister-group relationship either to each other or to any South American species.
4. *Leptodactylus silvanimbus* is known only from one small region of former cloud forest habitat in Honduras.

These patterns could follow a time line of differentiation, with *Leptodactylus fuscus* representing an Isthmian Link distributional extension into Middle America and, at the other extreme, *L. silvanimbus* being the only relictual remnant of the Middle American radiation in Savage's model (1982). Alternatively, *L. silvanimbus* in particular could represent a much more recent cladogenic event, from a common ancestor, with one of the other species of *Leptodactylus* that occur in Middle America.

To understand the zoogeographic history of *Leptodactylus* species in Middle America, we require a much better understanding of their relationships to each other and to all other *Leptodactylus* species. The advent of molecular techniques, in combination with nonmolecular data, gives some hope that it is possible to obtain much better knowledge of phylogenetic relationships among *Leptodactylus* species than is currently available.

In this chapter, we discuss preliminary results by focusing on the relationships of *Leptodactylus silvanimbus* to understand why it has a distribution pattern that differs fundamentally from all other known species of Middle American *Leptodactylus.* Specifically, we are interested in using preliminary data we have gathered to test alternative hypotheses of relationships that have fundamentally different biogeographic correlates. Before framing the hypotheses, we briefly summarize the relationships of *Leptodactylus silvanimbus,* as currently

understood. When the species was first described, it could not be clearly allocated to any of the previously defined species groups of *Leptodactylus* (McCrainie et al. 1980). Since then, on the basis of additional data, *L. silvanimbus* has been included as a member of the *Leptodactylus melanonotus* species group (McCrainie et al. 1986; Heyer et al. 1996) or as part of a *L. melanonotus-ocellatus* species group clade (Larson and de Sá 1998). Furthermore, a cladistic analysis of nonmolecular data for a set of taxa that included *L. silvanimbus* demonstrated that the species was a member of the genus *Leptodactylus* but that its relationships to other species in the *L. melanonotus* species group were not conclusive (Heyer 1998). The three hypotheses we wish to test are basically alternative responses to the question Is *L. silvanimbus* a member of the *L. melanonotus* species group?

Hypothesis 1. *Leptodactylus silvanimbus* is a member of the *L. melanonotus* species group that shared a most recent ancestor with *L. melanonotus* itself. If this hypothesis is true, it suggests that the common ancestor of the two species crossed a water barrier from South America to Middle America at some point from the time ancestors of the Middle American radiation were in place to before formation of the Isthmian Link.

Hypothesis 2. *Leptodactylus silvanimbus* is a member of the *L. melanonotus* species group but does not have a sister-group relationship with *L. melanonotus.* This hypothesis suggests that *L. melanonotus* and *silvanimbus,* or their respective ancestors, made independent entries into Middle America from South America, probably before formation of the Isthmian Link but after the ancestors of the Middle American radiation were in place.

Hypothesis 3. *Leptodactylus silvanimbus* does not demonstrate a sister-taxon relationship to any *Leptodactylus* species, including members of the *L. melanonotus* species group. This hypothesis suggests that *L. silvanimbus* is an old species with a relictual distribution, specifically a part of the Middle American radiation in the Savage (1982) model. It would likely not have a close relationship with any other species of *Leptodactylus.*

Materials and Methods

CHOICE OF TAXA

Previous phylogenetic results that included *Leptodactylus silvanimbus* indicated that on the basis of morphological, ecological, and behavioral data (Heyer 1998) and preliminary molecular data for 12S and 16S mitochondrial segments (R. de Sá and W. R. Heyer, unpub. data), the closest relatives of *L. silvanimbus* were members of the *L. melanonotus* and *ocellatus* groups. These same studies demonstrated that members of the genus *Physalaemus* serve as an appropriate outgroup to *Leptodactylus* for phylogenetic analyses.

One of the hypotheses we wish to test is that of a sister-group relationship between *Leptodactylus melanonotus* and *L. silvanimbus.* Beyond these two taxa, we include several other members of the *L. melanonotus* and *L. ocellatus* groups in our inquiry. Because of data availability, we include *L. podicipinus* (*melanonotus* group) and *L. bolivianus, chaquensis,* and *ocellatus* (*ocellatus* group). One member of the *L. fuscus* group (*L. latinasus*) and two members of the *L. pentadactylus* group (*L. pentadactylus* [see next paragraph], *L. rhodomystax*) are included as well. We used *Physalaemus gracilis* as our outgroup taxon because we have complete 12S and 16S sequence data comparable to our *Leptodactylus* data.

As the manuscript was being finalized for submission, WRH realized that he had assumed that a tissue sample of *Leptodactylus pentadactylus* from Peru was the source of the sequence data that RdS had sent to him just prior to RdS leaving on an extensive field trip, rather than a tissue sample from Panama. The nonmolecular data are for the Middle American population. Although the Amazonian and Middle American populations of *L. pentadactylus* represent different species (U. Galatti, pers. comm.), for the purposes of this chapter the results would not change if all the data had come from one or the other of the geographic entities involved.

NONMOLECULAR DATA

Most of the characters used in this analysis are those used previously (Heyer 1998). However, most earlier studies attempted to analyze relationships at the species-group level and higher. We also included color pattern characters and morphometric measurements.

For this study, 51 nonmolecular data characters were screened for phylogenetic analysis (see appendix 4.1 for voucher specimens). Three characters lacked information for three or more of the taxa. Five characters did not vary among the ten taxa. Four characters had a single different state that occurred only in one of the in-group taxa, thus providing no phylogenetic information. The remaining 39 character states are defined in appendix 4.2, following the definitions and rationale used previously (Heyer 1998), except for measurement characters, which are treated in the following paragraph.

The overall approach for defining character states of measurement variables is that described by Thiele (1993). The data for snout-vent length (SVL), head length/SVL, head width/SVL, eye-nostril distance/SVL, tympanum diameter/SVL, thigh length/SVL, shank length/SVL, and foot length/SVL were analyzed separately by sex. None of the measurement characters had equal variances, even when the data were log or log + 1 transformed. Log transformation resulted in most measurement data having lowest *F*-values in the ANOVA analyses and were used in character definition. For the measurement data to be comparable to the other data, we made an a priori decision to recognize no

Table 4.1 Analytic results used to determine the number of states per character for measurement characters

Log-transformed data	Males	Females
SVL	90	91
Head length/SVL	3	3
Head width/SVL	4	3
Eye-nostril distance/SVL	2	2
Tympanum diameter/SVL	2	3
Thigh length/SVL	3	3
Shank length/SVL	3	4
Foot length/SVL	3	3

Note: Values are ranges of log-transformed variables divided by the mean of coefficient of variation for all 10 taxa.

more than three character states per measurement character. To determine whether to recognize two or three states per character, we divided the range of the variable by the coefficient of variation for the variable (table 4.1). The results indicate that SVL potentially contains more phylogenetic information than the other measurement characters. Consequently, three states were recognized for SVL and two states for all the other characters. The Thiele (1993) procedure uses a formula that results in numbers that are then rounded to the nearest whole number, which represents that taxon's state. Most taxa had the same state for both sexes. In cases in which there was a different state number for the same species, if the differences between the values resulting from the Thiele (1993) formula were greater than .05, both states were included in the data set. For those cases in which the two states differ by less than .05, the value requiring the least modification to change the whole number assignment was used in order to recognize a single state for the character involved. The characters and states involved in this manipulation are as follows: head length/SVL for *Leptodactylus silvanimbus*, male 0, female 1 → 0; tympanum diameter/SVL for *L. melanonotus* and *podicipinus*, male 1, female 0 → 0; shank/SVL for *L. latinasus, rhodomystax, silvanimbus*, male 1, female 0 → 0; and foot/SVL for *L. podicipinus*, male 1, female 0 → 0.

The distribution of character states is shown in table 4.2.

MOLECULAR DATA

Tissue samples were obtained from the specimens listed in appendix 4.1. The DNA extraction procedure followed Hillis et al. (1996). Two segments of the mitochondrial genome were amplified using polymerase chain reaction (PCR).

Table 4.2 Distribution of character states for nonmolecular data used in phylogenetic analyses

	1	2	3	4	5	6	7	8	9	10	11	12	13
P. gracilis	3	1	3	0	0	1	0	0	0	0	0	0	0
L. rhodomystax	2	0	1	1	0	0	1	2	0,2	1	1	1	0
L. chaquensis	1	0	2	3	2	0	0	0	0	1	0	0	0
L. latinasus	2	0	0	0,3	0	0	0,1	1	0	0	1	0	1
L. bolivianus	0	0	1	2	2	0	0,1	0	0	1	1	0	1
L. pentadactylus	0,3	0	1	1	0	0	0	0	0,1	2	1	1	0
L. podicipinus	0,1	0	2	1	2	0	0,1	0,1	2	0	0	0	1
L. silvanimbus	0	0	2	0	1	0	0,1	0	0	0,1	0	0	0
L. melanonotus	0	0	2	0	2	0	0,1	0	0	0	1	0	0,1
L. ocellatus	0	0	2	3	2	0	0,1	0	0,1	1	0	0	0

	14	15	16	17	18	19	20	21	22	23	24	25	26
P. gracilis	0	0,1	1	1	2	0	0	0	0	1	1	1	0
L. rhodomystax	1	1	0	0	1	1	0	1	1	0	0	0	1
L. chaquensis	1	0,1	0	0	1	1	1	1	1	0	0	0	0
L. latinasus	1	0	0	0	0	0	0	1	1	1	1	0	0
L. bolivianus	0	1	1	1	0	1	1	1	1	0	0	0	0
L. pentadactylus	0	1	0	0	0	1	2	1	1	0	0	0	1
L. podicipinus	0	0,1	0	0	1	1	0	1	1	0	0	0	0
L. silvanimbus	0	1	0	1	1	1	0	1	1	0	0	0	0
L. melanonotus	0	0,1	0	0	1	1	0	1	1	0	0	0	0
L. ocellatus	1	0,1	0,1	0	1	1	1	1	1	0	0	0	0

	27	28	29	30	31	32	33	34	35	36	37	38	39
P. gracilis	1	1	0	0	0	0	0	0	0	4	0	3	1
L. rhodomystax	0	0	1	1	1	0	1	1	3	1	0	1	0
L. chaquensis	0	0	1	0	1	0	0	2	3	0,3	1	1,3	0,1
L. latinasus	0	0	1	0	0	1	2	1	0	2	0	0	0
L. bolivianus	0	0	1	0	1	1	0	2	0	0	1	1	0
L. pentadactylus	0	0	1	1	1	0	1	1	3	2	1	2	0
L. podicipinus	0	0	1	0	0	1	0	1	2	1	0	0	0,1
L. silvanimbus	0	0	1	1	0	0	0	1	4	0	0,1	1	1
L. melanonotus	0	0	1	0	0	0	0	1	1	1	0	0	0
L. ocellatus	0	0	1	0	1	1	1	1	4	0	1	2	1

Note: See appendix 4.2 for definition of characters and states.

A segment of the 12S rRNA of ~350 base pairs (bp) was amplified using primers 12Sa (5′-AAACTGGGATTAGATACCCCACTAT-3′) and 12Sb (5′-GAGGGTGACGGGCGGTGTGT-3′). A segment of the 16S rRNA of ~500 bp was amplified using primers 16SaR (5′-CGCCTGTTTACCAAAAACAT-3′) and 16Sd (5′-CTCCGGTCTGAACTCAGATCACGTAG-3′). Primer sequences were obtained from Reeder (1995). Double-stranded PCR amplifications were performed in a final volume of 50 µl containing 0.4 µl of each primer, 1.0 µl of each dNTP, 3.0 µl of 25 mM MgCl, and 1.25 units of Taq (*Thermus aquaticus*) DNA polymerase; the reaction was overlaid with 50 µl of mineral oil. PCR conditions were as follows: 94°C for 60 s, 57°C for 60 s, and 72°C for 60 s, with 25 cycles for the 12S amplification and 30 cycles for the 16S amplification. Purification of double-stranded amplified product was performed using Wizard PCR Preps Kit (Promega). Of the purified double-stranded fragment, 0.5 µl were mixed with 1.5 µl of a single IRD-labeled primer, 7.2 µl of sequencing buffer, 1 µl of Sequitherm Excel II (Epicentre Technologies Co.) DNA polymerase, and 6.8 µl of dH_2o. Subsequently, 4.0 µl of this mixture was added to each of four tubes containing 2 µl of each nucleotide, respectively. The PCR conditions were as follows (30 cycles): 92°C for 30 s, 55°C for 30 s, and 70°C for 30 s. The single-strand-amplified and infrared-labeled fragments were sequenced in a LI-COR 4200 IR DNA sequencer on 6% acrylamide gels.

Most of the 892 nucleotide positions were easily aligned. Eighty positions had ambiguous alignments and were not used in the phylogenetic analyses (contact authors for aligned sequences).

DATA ANALYSES

The 12S and 16S data are examined for nucleotide substitution saturation by plotting the number of transition changes and number of transversion changes against the total number of nucleotide changes, because we have no reliable information from the fossil record to time date cladogenic events in our data set.

Phylogenetic analyses were conducted using PAUP* test version 4.0a for Macintosh (Swofford 1999).

Four substitution models for the molecular data were explored: Jukes-Cantor (Jukes and Cantor 1969), Kimura two-parameter (Kimura 1980), Hasegawa-Kishino-Yano (Hasegawa et al. 1985), and the general time reversible (REV of Yang 1994a) (see Swofford et al. 1996 for model descriptions). Each substitution model was evaluated assuming (1) no rate heterogeneity among sites; (2) heterogeneity parameter I of Hasegawa et al. (1985), in which a proportion of sites was considered invariable; (3) heterogeneity parameter gamma (Γ) of Yang (1994b), in which all sites follow a discrete gamma distributed rates model; and (4) heterogeneity parameters I + Γ (Gu et al. 1995; Waddell and Penny 1996), in which some sites are considered invariable and variable sites follow a gamma distributed rates model. Rate heterogeneity parameters were optimized under each substitution model: 16 models were tested for both the 12S and 16S, and the 12S and 16S data combined. The likelihood ratio test (Sokal and Rohlf 1969) was used to determine whether models differed significantly in their likelihood scores.

Whether the 12S and 16S data sets should be combined for phylogenetic analysis was examined through two tests: (1) the partition-homogeneity test in PAUP* with heuristic search; and (2) the likelihood ratio test using the best substitution + heterogeneity model for the 12S and 16S data, where χ^2 (approximation) = 2 (−Ln likelihood of 12S + 16S data combined − (−Ln likelihood of 12S data + −Ln likelihood of 16S data)) and the degrees of freedom are equal to the branch lengths ($2T - 3$, where T = number of terminal taxa) + number of substitution model parameters.

The morphological data set was analyzed using maximum parsimony; the molecular data were analyzed using maximum likelihood, with the substitution and heterogeneity models that best fit the data. The morphological data were analyzed with exhaustive search settings. The maximum likelihood analyses were run only with heuristic search settings, because any other search setting took an unacceptable length of time to process (on a Macintosh G4 computer).

All phylogenetic analyses used *Physalaemus gracilis* as the outgroup to provide rooting information.

Results

NUCLEOTIDE SUBSTITUTION SATURATION

The number of transition and transversion changes plotted against the total number of nucleotide changes shows a straight-line relationship for the 16S data (fig. 4.1). The same plots for the 12S data suggest that saturation of transitional changes is present (fig. 4.2). The plot of transversional changes of the 12S data, although not a straight-line relationship, does not give any indication of saturation. Thus, of the two molecular data sets, the 16S data would be expected to resolve older cladogenic events better than the 12S data.

The percentages of nucleotide substitutions for 12S range from 11% to 15% for pair-wise comparisons between *Physalaemus gracilis* and the other species of *Leptodactylus* and from 4% to 12% for pair-wise comparisons among *Leptodactylus* species. The data for 16S are 11%–14% and 3%–11%, respectively.

MOLECULAR MODEL PARAMETERS

Of the 16 substitution and heterogeneity model combinations evaluated, the most complex model gave the best likelihood scores for both the 12S and 16S

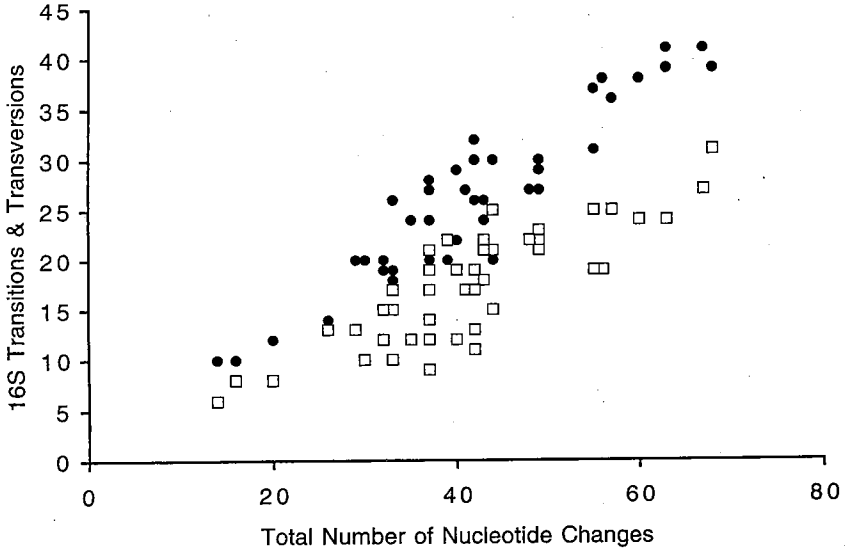

Figure 4.1 Nucleotide changes for 16S data. Filled circles indicate transitions; open squares indicate transversions.

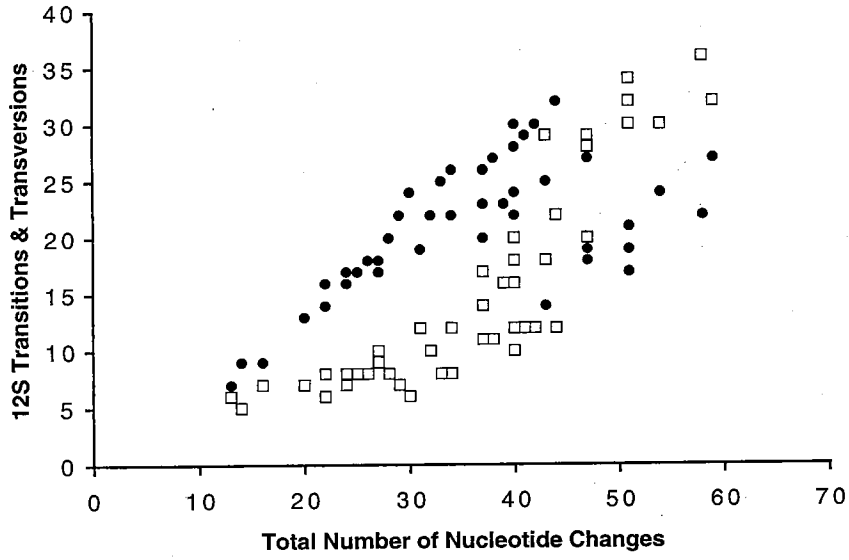

Figure 4.2 Nucleotide changes for 12S data. Filled circles indicate transitions; open squares indicate transversions.

Table 4.3 Likelihood ratio test data for 16 models of molecular evolution

	−Ln likelihood scores		
Model	12S data	16S data	12S + 16S data
JC	1,507.28810	1,895.84292	3,458.99269
JCΓ	1,437.17529	1,809.70338	3,280.90917
JCI	1,439.33569	1,811.45147	3,286.83392
JCI + Γ	1,435.64859	1,807.73041	3,274.52011
K2P	1,481.29020	1,867.32641	3,398.22787
K2PΓ	1,405.98660	1,778.23084	3,212.03986
K2PI	1,408.84496	1,780.13326	3,218.70940
K2PI + Γ	1,403.69033	1,775.53341	3,204.43102
HKY	1,472.70983	1,860.28960	3,387.66330
HKYΓ	1,395.63329	1,768.37781	3,198.73584
HKYI	1,399.26067	1,770.04109	3,205.63591
HKYI + Γ	1,392.81721	1,765.73308	3,190.71719
GTR	1,448.25768	1,843.66716	3,366.63289
GTRΓ	1,374.73904	1,756.60852	3,181.66991
GTRI	1,378.37353	1,758.93003	3,188.24311
GTRI + Γ	1,373.94599	1,753.93739	3,174.97869

Note: JC, Jukes-Cantor model; K2P, Kimura two-parameter model; HKY, Hasegawa-Kishino-Yano model; GTR, general time reversible model; Γ, heterogeneity parameter gamma; I, heterogeneity parameter I; I + Γ, heterogeneity parameters gamma and I.

data (table 4.3). The best model is the general time reversible (GTR) model with heterogeneity parameters I + Γ, and its likelihood score differs statistically from all the other likelihood scores for the other 15 models for both the 12S and the 16S data.

DATA PARTITIONS

The partition-homogeneity test for the 12S and 16S data results in $p = .02$.

The likelihood ratio test using the likelihood scores for the GTR + I + Γ model (table 4.3) has an approximate χ^2 value of 94,119 ($p < .001$ with 27 degrees of freedom).

Both analytic methods yield the same result: the 12S and 16S data are best analyzed separately. Given the inappropriateness of combining the 12S and 16S data, the 12S, 16S, and nonmolecular data sets are analyzed separately.

PHYLOGENETIC RELATIONSHIPS

Nonmolecular Data

Exhaustive maximum parsimony analysis of the nonmolecular data set resulted in 2,027,025 trees evaluated, with a single shortest tree with a length of 90, a single longest tree with a length of 135, and a g_1 statistic of −.55. Twenty-seven characters are parsimony informative. The single most parsimonious tree of length 90 has a consistency index excluding uninformative characters of .40, a retention index of .54, and a re-scaled consistency index of .36.

Bootstrap analysis of 100 replicates using default settings in PAUP* results in a moderately resolved tree (fig. 4.3). This tree configuration is used to evaluate the three competing hypotheses.

Molecular Data

Bootstrap analysis of 100 replicates using the GTR + I + Γ model, otherwise with default settings in PAUP* for the 16S data, yielded a completely unresolved tree. Cunningham et al. (1998) indicated that the most complex best-fit maximum likelihood models do not necessarily identify the correct phylogenetic tree. On the basis of analyses of 12S and 16S data in general, two model features seem most important in analyzing these data: (1) separation of transition and transversion parameters into separate classes; and (2) incorporation of the invariable sites parameter. The simplest model that incorporates these features is the Hasegawa-Kishino-Yano (HKY) + I model; the GTR + I model is more complex but contains these two features. For both the 12S and 16S data, bootstrap analyses using 100 replicates were run for the (1) HKY + I, (2) GTR + I, and (3) GTR + I + Γ models.

The 12S data have 51 parsimony-informative characters (estimated from maximum parsimony analysis of the data). All three models resulted in the same partially resolved tree topology (fig. 4.4).

The 16S data have 67 parsimony-informative characters (estimated from maximum parsimony analysis of the data). Both the GTR + I and GTR + I + Γ models yielded completely unresolved trees at 50% level of support. The HKY + I model yielded a partially resolved tree with rather poor support for the few clades that were supported with more than 50% support (fig. 4.5).

Evaluation of Hypotheses

Hypothesis 1. *Leptodactylus silvanimbus* and *L. melanonotus* are sister species. None of the data sets supports this hypothesis. Two of the three data sets do

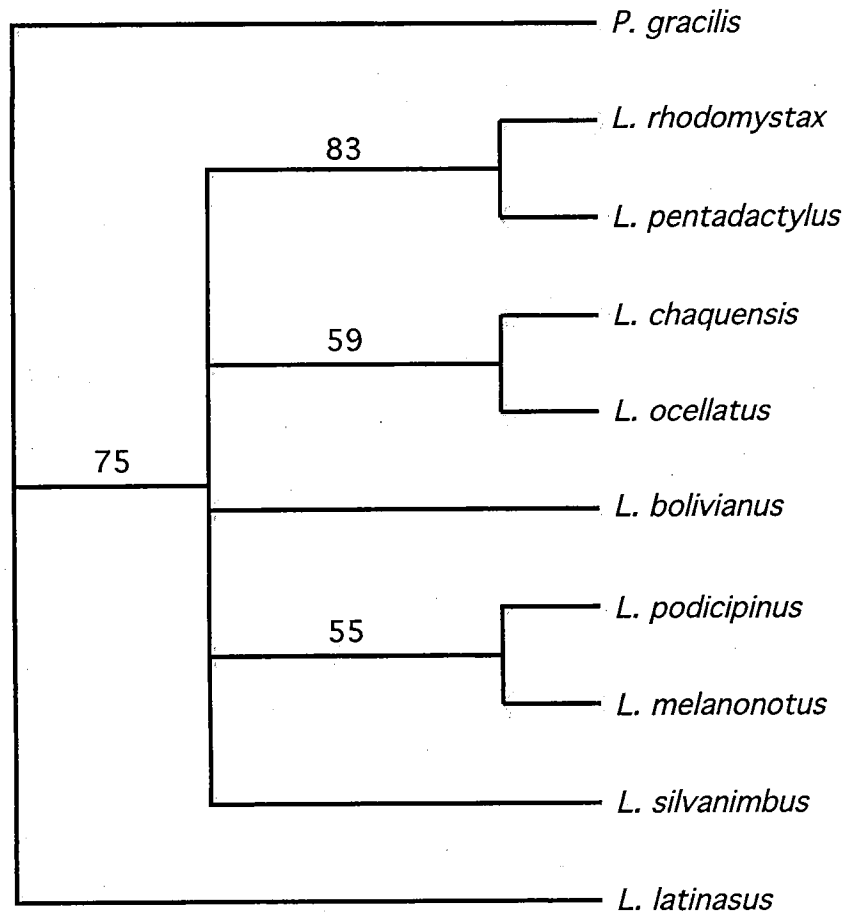

Figure 4.3 Results of parsimony analysis of primarily morphological characters. Numbers indicate bootstrap analysis results.

support a sister-group relationship for *L. melanonotus* and *L. podicipinus* for the taxa analyzed. The results of phylogenetic analysis of the three data sets lead to rejection of this hypothesis.

Hypothesis 2. *Leptodactylus silvanimbus* is a member of the *L. melanonotus* species group. For this hypothesis to be supported by the data, a clade comprising *L. melanonotus, L. podicipinus,* and *L. silvanimbus* in the data set analyzed would have to be recognized. In none of the data partitions is there

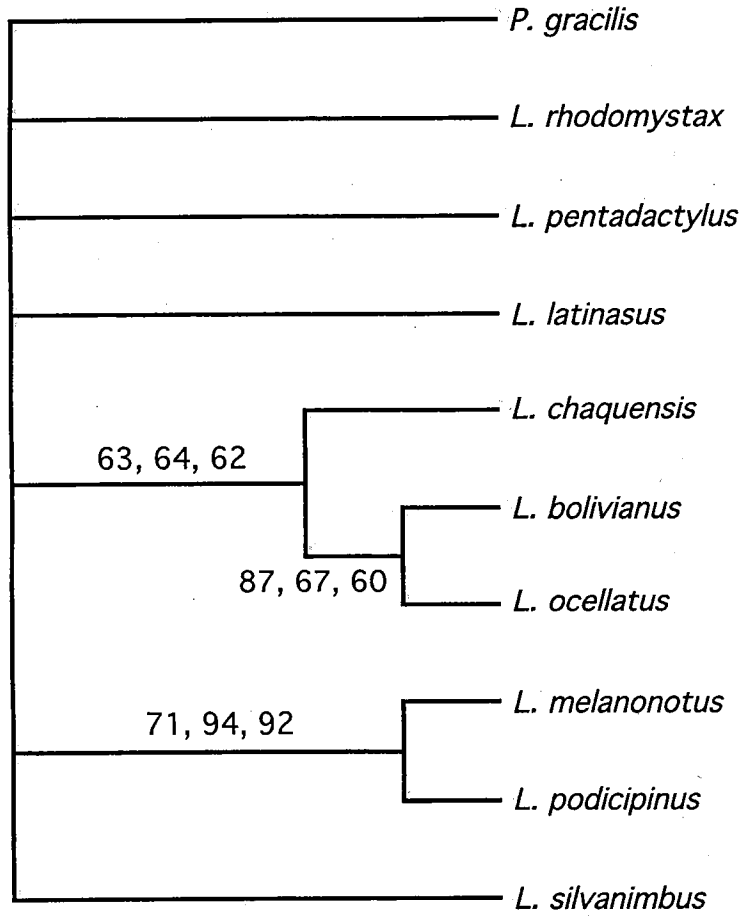

Figure 4.4 Results of maximum likelihood analyses of 12S data. Numbers indicate bootstrap analysis results for HKY + I, GTR + I, and GTR + I + Γ models, respectively.

bootstrap support for this clade at greater than 50% occurrence. In the morphological data set, this clade was found in only 5.5% of the bootstrap replicates. None of the molecular analyses found support for this clade at greater than 5% occurrence. The data are consistent with rejection of this hypothesis.

Hypothesis 3. *Leptodactylus silvanimbus* does not have a close relationship to other species of *Leptodactylus*. The three data partition results are consistent with this hypothesis. Therefore, of the three hypotheses, this one is best supported by our preliminary data.

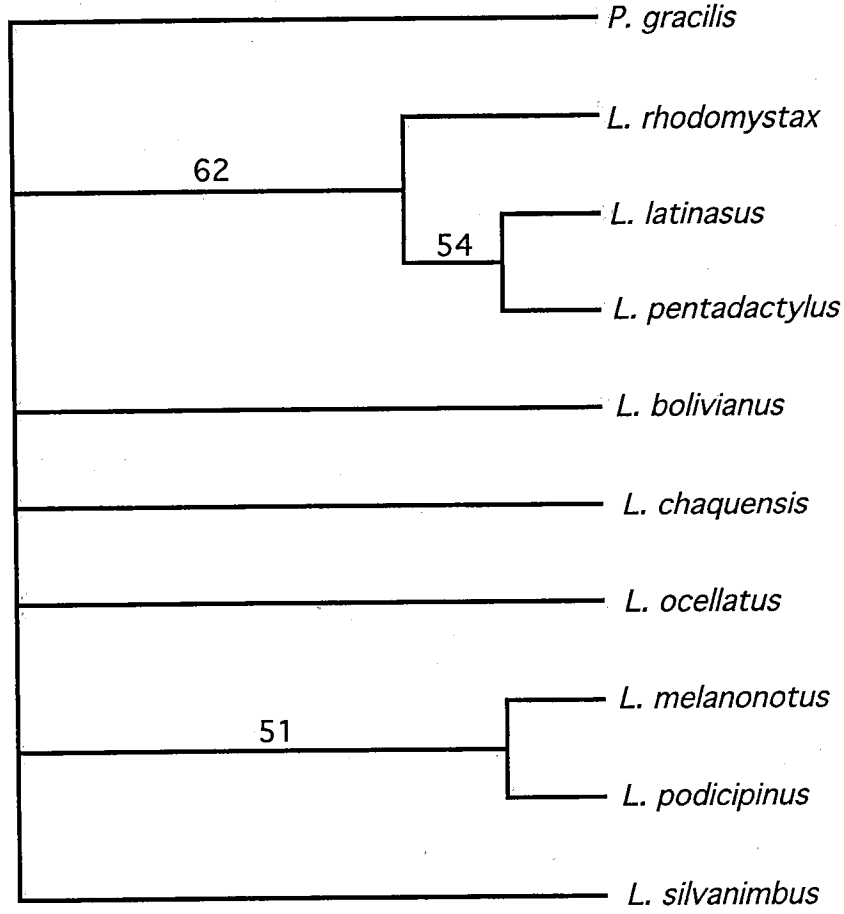

Figure 4.5 Results of maximum likelihood analysis of 16S data for the HKY + I model. Numbers indicate bootstrap analysis results.

We chose to analyze the three data sets separately for what we think are compelling reasons. We recognize that there are arguments for a total evidence, combined data analysis approach. We would have performed combined analyses of our two molecular data sets had they been statistically compatible. Further, some authors argue that the incompatibility tests we used are unreliable for determining the appropriateness of whether to combine data partitions (e.g., Yoder et al. 2001). To evaluate the robustness of our results, we performed a maximum likelihood analysis of the combined three data partitions by using

the program in development by D. A. Swofford that applies a likelihood simulation to analyze nonmolecular data. The heuristic analysis resulted in two retained trees. In both of them, *Leptodactylus silvanimbus* demonstrates a basal trichotomy with *Physalaemus gracilis* and all the other *Leptodactylus* species. This result adds additional support to the third hypothesis.

Discussion

The molecular and morphological data are sufficient to demonstrate that if *Leptodactylus silvanimbus* and *L. melanonotus* shared a close sister-group relationship, such a relationship would have been identified. All data partitions strongly reject this hypothesis.

In contrast, additional data could indicate that the second hypothesis is correct rather than the third. Stronger differentiation between these two hypotheses would be facilitated by having strongly supported resolved trees, particularly basally. Our results indicate that although the 12S and 16S ribosomal DNA sequences may help us to understand species relationships, a more slowly evolving molecule is needed to resolve the earlier cladogenic events in the genus. Increasing the number of *Leptodactylus* taxa would increase our confidence in the phylogenetic results by decreasing random error (Swofford et al. 1996, 503). Resolution of relationships is generally better when the ratio of characters to taxa is high. Although there are additional morphological phylogenetically informative characters for *Leptodactylus* that could be added, at this point it is unlikely that we could double the number of such characters, and many of the additional characters would be unknown for many of the known species of *Leptodactylus*. Therefore, the most logical way to add a significant number of new characters to our data set would be through addition of new molecular sequences.

Until such additional data become available, however, the present data best support the conclusion that *Leptodactylus silvanimbus* is the only living member of the genus that is part of Savage's Middle American radiation. *Leptodactylus silvanimbus* currently occurs on the ancient Chortis Block landmass, which has been land positive since the Paleocene (see, for example, Iturralde-Vinent and MacPhee 1999 and references). How long *L. silvanimbus* has occupied the Chortis Block is unknown and likely knowable only if appropriately aged fossil deposits containing the species are discovered.

Appendix 4.1 Voucher Specimens

Tissue Vouchers

Leptodactylus bolivianus. USNM 268966 (USFS 152368). Peru: Madre de Dios; Tambopata Reserve. 12°50′ S, 69°17′ W.

Leptodactylus chaquensis. USNM 319708 (USFS 186524). Argentina: Tucumán; ~40 km southeast of San Miguel de Tucumán at km post 1,253 on International Route 9.

Leptodactylus latinasus. USNM 535969 (RdS 763). Uruguay: Paysandu; Parque Municipal "San Francisco." 34°31′ S, 56°24′ W.

Leptodactylus melanonotus. USNM 535964 (RdS 759). Belize: Cayo; San Jacinto and Spanish Lookout Road, between Webster Highway, Caesar's Hotel.

Leptodactylus ocellatus. USNM 535972 (RdS 755). Uruguay: Rocha; Rocha City, near Bañados de los Indios, Route 14, at 10 km from Route 9, Campo del Sr. Martin, Estancia La Palma Paraje.

Leptodactylus pentadactylus. USNM 268971 (USFS 152237). Peru: Madre de Dios; Tambopata Reserve. 12°50′ S, 69°17′ W.

Leptodactylus podicipinus. USNM 303207 (USFS 053124). Brazil: São Paulo; Fazenda Jatai. 21°33′ S, 47°43′ W.

Leptodactylus rhodomystax. MZUSP 70375 (940333). Brazil: Pará; Serra de Kukoinhokren.

Leptodactylus silvanimbus. USNM 348631 (LDW 10478). Honduras: Ocotepeque; Belen Gualcho. 1,600 m. 14°29′ N, 88°47′ W.

Physalaemus gracilis. RdS 788. Uruguay: Salto; Espinillar.

Morphological Vouchers

The following specimens examined for this study supplement those examined previously (Heyer 1998).

WET METAMORPHOSED SPECIMENS

Physalaemus gracilis. USNM 539179. Pozos Azules, Sierra de Animas, Maldonado, Uruguay (male; jaw, throat, and thigh muscles examined).

DRY SKELETONS

Leptodactylus bolivianus. USNM 298939. Cuzco Amazonico, Río Madre de Dios, Madre de Dios, Peru (female).

L. chaquensis. USNM 227604. Near Embarcación, Salta, Argentina (male).

L. ocellatus. USNM 342484. San Lorenzo, Central, Paraguay (male).

L. pentadactylus. USNM 539175. Igarapé Belém, Amazonas, Brazil (male). USNM 539395. Porto Velho, Rondônia, Brazil (sex unknown, skull only).
L. podicipinus. USNM 297780. Estancia Caiman, Mato Grosso do Sul, Brazil (female).
L. rhodomystax. USNM 539176. Igarapé Belém, Amazonas, Brazil (sex unknown).

CLEARED AND STAINED SPECIMENS

Leptodactylus latinasus. USNM 227578. Artilleros, Colonia, Uruguay (male).
L. ocellatus. USNM 227598. Near Monte Grande, Buenos Aires, Argentina (juvenile female).
Physalaemus gracilis. USNM 539179. Pozos Azules, Sierra de Animas, Maldonado, Uruguay (male).

Appendix 4.2 Character State Definitions for Nonmolecular Data

See Heyer 1998 for further clarification of state definitions and ordering rationale.

1. Vocal sac: state 0, no vocal sac visible externally but present internally; state 1, indications of lateral vocal folds; state 2, well-developed paired lateral vocal sacs; state 3, well-developed large, single vocal sac. Character states analyzed unordered because PAUP* does not allow multistate taxa for ordered characters.

2. Tympanum visibility: state 0, tympanum well developed, easily seen externally; state 1, tympanum concealed, not visible externally.

3. Male thumb spines: state 0, thumb without modifications; state 1, thumb with one horny spine; state 2, thumb with two horny spines; state 3, thumb with nuptial pads. Character states analyzed unordered because PAUP* does not allow multistate taxa for ordered characters.

4. Dorsolateral folds: state 0, no folds; state 1, 1 short pair; state 2, 1 well-developed pair; state 3, 3–5 well-developed pairs. The state ordering is 0-1-2-3.

5. Toe webbing: state 0, no web or fringe; state 1, weak basal fringes and webbing; state 2, toes with lateral fringes extending length of toes except for tips. The state ordering is 0-1-2.

6. Tarsal decoration: state 0, tarsal fold; state 1, tarsal tubercle and fold.

7. Lip pattern: state 0, upper lip lacking a distinct light stripe; state 1, upper lip with distinct light stripe.

8. Pattern on posterior thigh: state 0, uniform or mottled; state 1, distinct light stripe on lower portion of posterior thigh; state 2, distinct light spots. Character states analyzed unordered.

9. Belly pattern: state 0, light and/or indistinctly mottled; state 1, distinct bold or anastomotic mottle; state 2, dark with ill- to moderately defined light spots. Character states analyzed unordered.

10–17. Measurement data for SVL (10), head length/SVL (11), head width/SVL (12), eye-nostril distance/SVL (13), tympanum diameter/SVL (14), thigh/SVL (15), shank/SVL (16), and foot/SVL (17). See "Materials and Methods." Character 10 state ordering is 0-1-2.

18. Larval head/body pattern: state 0, uniform and light; state 2, uniform and dark; state 3, mottled. Character states analyzed unordered.

19. Larval tail pattern: state 0, mottled; state 1, rather uniform, pigmented or not.

20. Larval tooth rows: state 0, 2(2)/3 or 2(2)/3(1); state 1, 2/3 or 2/3(1); state 2, 1/2(1). These character states eliminate intraspecific variation in this data set. Character states analyzed unordered.

21. Larval vent position: state 0, dextral; state 1, medial.

22. Depressor mandibulae: state 0, DFSQat; state 1, DFsq or DFsqat.

23. Geniohyoideus medialis: state 0, muscle continuous medially, dividing posteriorly where the posteromedial processes of the hyoid articulate with the body of the hyoid, hyoglossus muscle completely covered ventrally by the geniohyoideus medialis; state 1, muscle divided ventrally, exposing hyoglossus, posterior half of muscle covered ventrally by sternohyoideus.

24. Geniohyoideus lateralis: state 0, no attachment of muscle to hyale; state 1, distinct slip attaches to hyale anterolaterally.

25. Anterior petrohyoideus: state 0, insertion entirely on edge of hyoid apparatus; state 1, insertion entirely on ventral surface of hyoid body.

26. Sternohyoideus origin: state 0, single medial slip originates from meso- and xiphisterna; state 1, medial slip divides in two slips, one originating from anterior portion of mesosternum, another from the posterior meso- and/or xiphisternum.

27. Sternohyoides insertion: state 0, in narrow band near lateral edges of hyoid; state 1, in a narrow band with fibers attached near midline posteriorly.

28. Omohyoideus: state 0, insertion partly on hyoid plate and partly on fascia between the posterolateral and posteromedial processes of the hyoid; state 1, muscle inserts entirely on hyoid plate ventrally.

29. Iliacus externus: state 0, short state of Limeses (1964); state 1, long B state of Limeses (1964).

30. Sartorius: state 0, moderate; state 1, broad.

31. Posterolateral projection of frontoparietal: state 0, no or minimal projection; state 1, distinct projection.

32. Anterior articulation of vomer: state 0, no articulation or overlap with

premaxilla or maxilla; state 1, articulation or overlapping with premaxilla or maxilla.

33. Sphenethmoid and optic foramen relationship: state 0, posterior extent of sphenethmoid widely separated from optic foramen; state 1, posterior extent of sphenethmoid closely approximates optic foramen; state 2, posterior extent of sphenethmoid borders optic foramen. The state ordering is 0-1-2.

34. Pterygoid-parasphenoid overlap: state 0, no overlap in an anterior-posterior plane; state 1, elements overlap but are not in contact; state 2, elements overlap and are in contact. The state ordering is 0-1-2.

35. Advertisement call pulse structure: state 0, single pulse; state 1, each note with 2 consistent, well-defined pulses; state 2, each note with 2–5 strong pulses, one or more of the strong pulses partially pulsed; state 3, each note of more than 6 pulses; state 4, entire note partially pulsed. State 4 unordered; remaining state ordering 0-1-2-3.

36. Call frequency modulation: state 0, none or negligible; state 1, rising frequency modulation, extremely sharp; state 2, rising frequency, moderate; state 3, rising and falling frequencies throughout call; state 4, falling frequencies throughout call. Character states analyzed unordered.

37. Carrier frequencies: state 0, most or all $>$ 1,000 Hz; state 1, most or all $<$ 1,000 Hz.

38. Call duration: state 0, $<$ 0.1 s; state 1, 0.1–0.2 s; state 2, 0.2–0.5 s; state 3, $>$ 0.5 s. Character states analyzed unordered because PAUP* does not allow multistate taxa for ordered characters.

39. Harmonic structure: state 0, none or weak; state 1, distinct.

Acknowledgments

Without James R. McCranie and Larry David Wilson, this report would not have been possible. Their field experience and expertise provided the tissue samples of *Leptodactylus silvanimbus* so that molecular analyses could be performed. The following individuals either provided other tissue samples or facilitated our collecting of same: Andrew Chek, Reginald B. Cocroft III, Ronald I. Crombie, Esteban O. Lavilla, Alejandro Olmos, and Addison Wynn. Dr. P. E. Vanzolini graciously responded to a request for skeletal material of *Leptodactylus pentadactylus* and *L. rhodomystax* by preparing skeletons of those species for this analysis.

WRH thanks the following colleagues at the National Museum of Natural History for their patience in responding to a continuous stream of questions and for the help they provided regarding molecular data and their analyses: Kevin de Queiroz, Jon Norenburg, and James Wilgenbusch.

This research was supported by grants from the F. Jeffress and Kate Miller Memorial Trust (grant J-450 to RdS), the Virginia Academy of Sciences, the Neotropical Lowlands Research Program, Smithsonian Institution (Richard P. Vari, principal investigator), and the National Science Foundation (award 9815787 to RdS and WRH).

Ecology & Evolution in the Tropics

A Herpetological Perspective

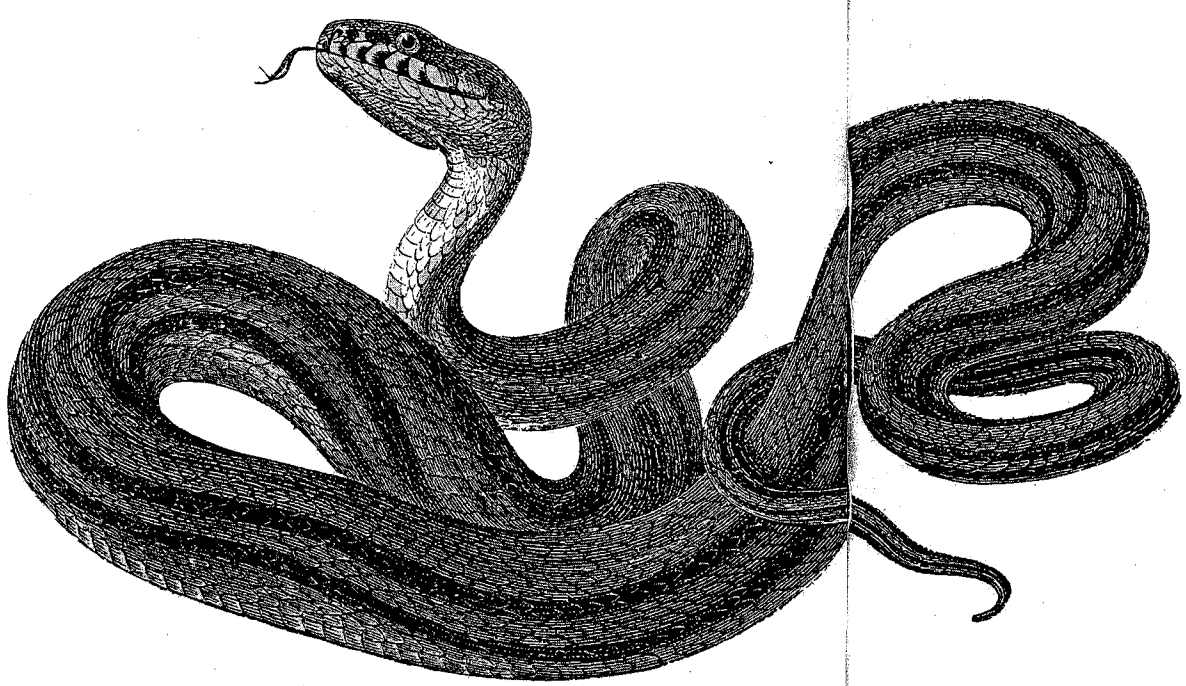

Edited by Maureen A. Donnelly,
Brian I. Crother, Craig Guyer, Marvalee H. Wake,
& Mary E. White

The University of Chicago Press • *Chicago & London*

Maureen A. Donnelly *is associate professor of biology at Florida International University.* ***Brian I. Crother*** *is professor of biological sciences at Southeastern Louisiana University and the editor of* Caribbean Reptiles. ***Craig Guyer*** *is professor of biology at Auburn University.* ***Marvalee H. Wake*** *is professor emerita of integrative biology at the University of California, Berkeley, and the editor of* The Origin and Evolution of Larval Forms *and* Hyman's Comparative Vertebrate Anatomy, *published by the University of Chicago Press.* ***Mary E. White*** *is professor of biological sciences at Southeastern Louisiana University.*

The University of Chicago Press, Chicago 60637
The University of Chicago Press, Ltd., London

Printed in the United States of America

14 13 12 11 10 09 08 07 06 05 1 2 3 4 5

ISBN: 0-226-15657-5 (cloth)
ISBN: 0-226-15658-3 (paper)

Library of Congress Cataloging-in-Publication Data

Ecology and evolution in the tropics : a herpetological perspective / edited by Maureen A. Donnelly . . . [et al.].
p. cm.
Includes bibliographical references and index.
ISBN 0-226-15657-5 (cloth : alk. paper) — ISBN 0-226-15658-3 (pbk. : alk. paper)
1. Amphibians—Ecology—Tropics. 2. Reptiles—Ecology—Tropics.
3. Amphibians—Evolution—Tropics. 4. Reptiles—Evolution—Tropics.
I. Donnelly, Maureen A., 1954–
QL664.6.E36 2005
597.9'1734'0913—dc22

2004014642

This book is printed on acid-free paper.

To the memory of James Edward DeWeese,
David Joseph Morafka, & Joseph Bruno Slowinski